

# Advanced in Ultra-High Field Task-Based fMRI

Author Alessandro Nigi<sup>1</sup> - 6358292

Supervisor Wietske van der Zwaag<sup>2</sup>

Examiner Alex Bhogal<sup>1</sup>

<sup>1</sup>Image Science Institute, University Medical Centre Utrecht, Utrecht, the Netherlands

<sup>2</sup>Spinoza Centre for Neuroimaging, Amsterdam, the Netherlands

## ABSTRACT

Task-based functional Magnetic Resonance Imaging (fMRI) at ultra-high field ( $\geq 7T$ , UHF) has revolutionized our understanding of the human brain by enabling investigations of brain activity during specific cognitive tasks with unprecedented precision. This review explores recent advancements in novel and advanced task-based UHF fMRI techniques that have expanded the scope of studying brain function, offering novel opportunities to explore neural responses and their relationship to cognitive processes, particularly in the context of laminar and columnar sub-millimetre fMRI. We discuss the most common Blood Oxygenation Level-Dependent (BOLD) fMRI methods and examine the strategies to address their limitations such as fast BOLD fMRI strategies, which include simultaneous multi-slice (SMS) acquisition, parallel imaging and line-scanning fMRI, which enable investigations of sub-millimetre scales with higher temporal resolution. The paper also presents insights into alternative contrast mechanisms like cerebral blood volume (CBV) imaging using vascular space occupancy (VASO) contrast and direct cerebral blood flow (CBF) measurements using arterial spin labelling (ASL). These techniques hold promise in studying specific cortical layers and columns, elucidating fine-scale neural structures and functional organization. These advancements in task-based UHF fMRI provide valuable insights into neural mechanisms underlying cognitive processes and pave the way for reliable mesoscopic resolution and sub-second temporal resolution in fMRI studies. As the field continues to evolve, integrating these cutting-edge techniques with advancements in hardware and post-processing methods will unlock even more detailed and comprehensive understandings of brain function, opening new horizons for cognitive neuroscience research.

## INTRODUCTION

Task-based functional Magnetic Resonance Imaging (fMRI) methods at ultra-high field ( $\geq 7T$ , UHF) have revolutionized our understanding of the human brain by enabling researchers to investigate brain activity during specific cognitive tasks in unprecedented detail<sup>1-5</sup>. In recent years, continuous research led to significant advancements in the development of task-based fMRI techniques, expanding the scope of studying brain function with improved precision and specificity<sup>6-10</sup>. These cutting-edge methods offer valuable opportunities to explore the complexities of neural responses and their relationship to cognitive processes.

To study task-based laminar and columnar activity, which are fundamental units of brain function, researchers often aim for resolutions of less than 1 mm in the imaging plane<sup>5,11</sup>. Some studies have pushed the resolution to as fine as 0.5 mm or even 0.3 mm, especially when using advanced MRI techniques and UHF systems<sup>5,11,12</sup>. Such high spatial resolution is necessary to capture the subtle differences in neural activity occurring at different depths of the cortex, providing insights into the organization of neural circuits and information processing across cortical layers and functional columns. However, as we will discuss, achieving such high resolution comes with technical challenges related to image quality, signal-to-noise ratio, and increased acquisition time, which researchers strive to overcome using innovative imaging strategies.

Here I will first introduce the Blood Oxygenation Level-Dependent (BOLD)<sup>13,14</sup> fMRI methods like gradient-echo (GE) echo planar imaging (EPI, GE-EPI)<sup>8,15</sup>, which, while widely used in task-based studies, has inherent limitations such as their indirect measure of neural activity and low functional specificity due to large

draining vessels bias. To overcome these limitations, researchers have explored alternative sequences and contrast mechanisms that complement or enhance the BOLD signal.

Temporal resolution plays a crucial role in capturing the dynamic nature of neural responses during cognitive tasks. In section 2, we discuss how the introduction of simultaneous multi-slice (SMS) acquisition and acceleration techniques based on parallel imaging has significantly improved the temporal resolution of task-based fMRI<sup>16-19</sup>.

Section 3 covers how line-scanning fMRI led to significant improvements in spatial resolution<sup>20-22</sup>. Line-scanning fMRI selectively excites thin slices of brain tissue, enhancing spatial precision and allowing researchers to investigate fine-scale neural structures and functional organization in greater detail.

In addition to advancements in spatiotemporal resolution, alternative contrast mechanisms have been developed to increase the specificity of the functional signal. Cerebral blood volume (CBV)<sup>9,23</sup> imaging using vascular space occupancy (VASO)<sup>24-26</sup> contrast offers a more comprehensive understanding of neurovascular dynamics during task-based experiments. Direct measurements of cerebral blood flow (CBF)<sup>9,27,28</sup> using arterial spin labelling (ASL)<sup>10,29</sup> techniques provide a more direct measure of neural activity, contributing to the investigation of cognitive processes. These alternative contrasts will be discussed in sections 4 and 5.

Finally, section 6 is dedicated to a few recent alternative acquisitions and contrasts. These methods consist of combinations and adaptations of the previously discussed strategies, demonstrating the vastity of choice the field offers to researchers to address a wide range of research questions.

## 1. BOLD-weighted fMRI at UHF

The most commonly employed technique for BOLD fMRI at UHF is GE-EPI.<sup>8,15</sup> This method utilizes rapidly switching gradients to acquire echo-planar images with short echo times (TE), enabling fast whole-brain coverage and high temporal resolution. The benefits of GE-EPI at UHF include increased Signal-to-Noise Ratio (SNR), allowing for improved spatial resolution and the detection of smaller BOLD signal changes<sup>12</sup>.

However, GE-EPI has several disadvantages that limit its reliability and applicability. These drawbacks include susceptibility artefacts, limited specificity in detecting the BOLD signal, and challenges in achieving high spatial resolution and precise localization<sup>12,30,31</sup>. Susceptibility artefacts are particularly problematic at tissue interfaces like air-tissue and bone-tissue boundaries, leading to signal dropout, distortions, and reduced image quality, especially in regions like the frontal and temporal lobes where susceptibility effects are prominent. These artefacts can hinder the accurate localization of functional activations and impact result interpretation. Another limitation of GE-EPI is its lack of specificity in distinguishing between extravascular and intravascular contributions to the BOLD signal. The BOLD signal is highly complex as it arises from changes in blood flow, blood volume, and blood oxygenation<sup>14,32</sup>. GE-EPI's inability to differentiate these contributions may lead to confounds in fMRI interpretation. Further, achieving high spatial resolution in fMRI is vital to localize functional activations within fine-scale structures like laminae and columns. However, this goal is challenging with GE-EPI due to factors such as acquisition speed, image distortions, and increased susceptibility artefacts at higher field strengths. Moreover, while EPI sequences offer relatively fast whole-brain coverage, they face limitations in achievable temporal resolution due to factors like repetition time (TR) and TE constraints. To improve temporal resolution, shorter TRs and TEs are desired, but they can exacerbate susceptibility artefacts and reduce SNR by limiting signal detection. Balancing the need for high temporal resolution with other considerations is crucial. Finally, UHF imaging also presents inherent challenges, including susceptibility artefacts and longer T2\* relaxation times, leading to signal dropout and image distortions.

Overall, GE-EPI is a widely used technique for BOLD fMRI at UHF due to its benefits in whole-brain coverage and temporal resolution. However, its disadvantages, such as susceptibility artefacts and limited specificity, severely limit its reliability and applicability. Researchers continue to address these challenges by developing advanced preprocessing methods and alternative sequences to enhance the quality and spatiotemporal resolution of BOLD fMRI data at UHF<sup>33</sup>.

For instance, Kashyap et al. introduced an alternative approach for laminar BOLD fMRI at 7T for mapping the cortical BOLD response with enhanced spatial precision, allowing direct examination of the mesoscopic organization of the human cortex<sup>34</sup>. The method involves employing highly anisotropic “pancake” voxels to sample

cortical depths, enabling focused investigation of cortical layers and columns. Comparing the depth profiles obtained using the anisotropic voxel approach (AVF) to the commonly used isotropic voxel encoding (IVE) in laminar studies, the study demonstrates the superior effective spatial resolution of AVF in two dimensions, although it comes at the cost of reduced brain coverage (Fig 1). By exploring the functional properties of AVF in studying cortical depth and distance profiles through simulations, the research establishes its advantage over IVE in terms of spatial resolution. Despite these benefits, the AVF approach has some limitations, such as its requirement for a relatively flat cortex with dimensions of approximately  $\sim 1.4 \text{ mm} \times 2 \text{ mm}$  and the necessity for prior knowledge of the subject's anatomy and approximate activation location. Nevertheless, the proposed technique offers exciting possibilities for investigating cortical layers and columns, providing valuable insights into the fine-grained organization of the human cortex and advancing our understanding of brain function at a more detailed spatial scale.

Further, multi-echo EPI has also emerged as a valuable technique in task-based BOLD fMRI studies<sup>35–37</sup>. This approach involves acquiring multiple echoes within a single echo train, capturing different points along the T2\* decay curve. Multi-echo EPI offers several advantages for task-based fMRI. Firstly, it provides an improved characterization of the BOLD signal by capturing different contrast-weighted images, allowing for the separation of BOLD and non-BOLD contributions. By fitting the acquired echoes to a biophysical model, such as the extended phase graph model, quantitative estimates of BOLD contrast, T2\*, and other parameters can be obtained, enhancing the specificity and interpretability of the fMRI results<sup>38,39</sup>. Secondly, multi-echo EPI allows for the detection and correction of artefacts associated with field inhomogeneities and susceptibility effects. Through the acquisition of multiple echoes, it becomes possible to estimate and correct for distortion and signal dropout caused by susceptibility artefacts, improving the overall image quality<sup>38,39</sup>. Finally, the acquired multi-echo data can be utilized to extract additional information about the underlying physiology, such as CBF and cerebral metabolic rate of oxygen consumption (CMRO2), by leveraging the T2\* and T2-weighted information<sup>40</sup>. These additional measures can provide complementary insights into the neurovascular coupling and metabolic demands of the activated regions during task-based fMRI experiments.

While multi-echo EPI offers several advantages for task-based BOLD fMRI, it also has some limitations to consider<sup>35,39,40</sup>. Firstly, acquiring multiple echoes within a single echo train increases the acquisition time, potentially reducing the temporal resolution of the fMRI data. Secondly, the acquisition of multiple echoes may lead to a decrease in the signal-to-noise ratio (SNR) compared to single-echo EPI, affecting the detectability of subtle BOLD signal changes<sup>21,36</sup>. Additionally, the processing of multi-echo EPI data can be more complex due to the need for separation and utilization of different echoes, and challenges in image registration and distortion correction

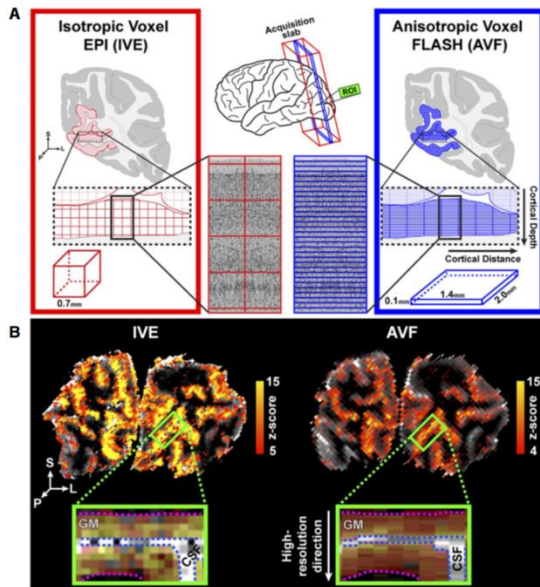


**Fig 1.** (A) Two distinct acquisition schemes for layer-specific fMRI: the IVE (left, red) and the novel AVF (right, blue) methods. This visual representation highlights the unique advantages of the AVF approach over the traditional IVE method in layer-specific fMRI. (B) Single-subject, single-run activation maps for flickering checkerboard stimulus in IVE (left) and AVF (right) acquisitions, revealing the region of interest (ROI) in a coronal slice through the occipital lobe. Zoomed-in panels show the grey matter-white matter (GM-WM) boundary (dotted pink line) and grey matter-cerebrospinal fluid (GM-CSF) border (blue line)<sup>34</sup>.

across the echoes. The use of multi-echo EPI introduces additional parameters and assumptions in the data analysis, which may pose a risk of confounding effects if not appropriately addressed<sup>37,40</sup>. Finally and most importantly, at 7T, the  $T_2^*$  of grey matter (25-28ms) is much shorter than at 3T (50ms). Consequently, to achieve comparable results, the same multi-echo readout must be compressed into a much shorter time for 7T imaging<sup>35,40</sup>. However, this poses challenges as it places greater strain on the gradients, and consequently, it also becomes more demanding on the volunteers due to the intensified acoustic noise experienced during the scanning process. Despite these disadvantages, careful consideration of acquisition strategies, preprocessing techniques, and data analysis methodologies can help mitigate these limitations and optimize the application of multi-echo EPI in task-based fMRI studies.

## 2. Fast BOLD fMRI

Advanced imaging sequences such as SMS BOLD fMRI and parallel imaging techniques have emerged as powerful approaches to increase both temporal and spatial resolutions in BOLD fMRI. SMS BOLD fMRI employs multi-band radio frequency (RF) pulses to simultaneously excite and acquire multiple slices within each TR<sup>17-19,41</sup>. The multi-band approach effectively reduces the duration of each TR, allowing for faster sampling of the fMRI time series. This time-saving advantage enhances temporal resolution, enabling the capture of faster brain dynamics. Further, by using the saved time, SMS allows to acquire

more k-space data, enabling to achieve higher spatial resolution imaging. This increased sampling rate and spatial resolution captures rapid changes in the BOLD signal of fine-scale structures, facilitating the investigation of fast-evolving neural processes at sub-millimetre scales<sup>17,19,41</sup>.

Moreover, parallel imaging techniques, such as sensitivity encoding (SENSE)<sup>42</sup> and generalized autocalibrating partially parallel acquisitions (GRAPPA)<sup>43,44</sup>, are employed in fMRI to overcome the inherent trade-off between spatial and temporal resolutions. These techniques exploit the spatial sensitivity profiles of the multiple receiver coil elements in the phased array coil setup to reconstruct data acquired with undersampled k-space trajectories. By doing so, parallel imaging techniques enable the acquisition of extremely high temporal resolution fMRI images. Particularly, SENSE utilizes the known spatial sensitivity maps to reconstruct the aliased data<sup>18,42</sup>, while GRAPPA estimates the missing k-space data by using the acquired calibration data<sup>18,43</sup>. These reconstruction methods effectively reduce image acquisition times and improve spatial resolution by mitigating the blurring effects caused by the extended point spread function. Consequently, parallel imaging techniques enhance the ability to resolve fine-scale spatial details and improve the localization of functional activations in fMRI studies.

In addition to SMS and parallel imaging techniques, three-dimensional (3D) EPI has emerged as a promising method to increase spatial resolution in task-based BOLD fMRI<sup>45,46</sup>. Traditional EPI acquires images in a slice-by-slice manner, leading to through-plane blurring and limitations in spatial resolution<sup>47</sup>. In contrast, 3D-EPI acquires volumetric data by sampling one plane of k-space per one or two shots. This approach allows for higher spatial resolution in all directions, capturing finer anatomical details and improving the ability to localize functional activations with greater precision. 3D-EPI sequences utilize segmented k-space acquisitions, with each segment encoding a portion of the 3D volume. These segments are then combined to reconstruct the complete volume. The use of 3D-EPI enhances the effective resolution along the phase-encoding direction and reduces the impact of through-plane blurring. However, this method also presents challenges, including longer echo trains that increase susceptibility-induced signal losses and distortions<sup>46,48</sup>. These challenges can be addressed through the integration of parallel imaging techniques. Additionally, multi-echo acquisitions can be employed with 3D-EPI to estimate and correct for BOLD signal distortions caused by susceptibility effects<sup>35-37</sup>. By combining 3D-EPI with these advanced techniques, researchers can achieve higher spatial resolution and improved image quality, leading to enhanced sensitivity in fMRI studies.

## 3. Line-scanning BOLD fMRI

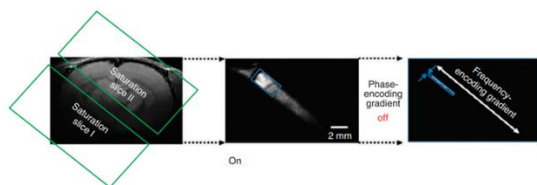


Fig 2. Set up of the line-scanning method<sup>51</sup>.

Line-scanning is an alternative approach used in BOLD fMRI studies that offer unique advantages compared to traditional volumetric imaging methods.<sup>20,49,50</sup> In line-scanning, rather than acquiring full 3D volumes, a single line or narrow strip of voxels is repeatedly sampled along a specific direction, typically through the cortex (Fig. 1). This sampling technique allows for high temporal resolution, as data from a single line can be acquired much faster compared to acquiring an entire 3D volume. The increased temporal resolution enables the tracking of rapid neural events with high precision. Additionally, line-scanning reduces the impact of physiological noise from cardiac and respiratory cycles, as it focuses on a smaller region of interest<sup>20,21</sup>. By targeting specific cortical layers or regions, line-scanning can provide insights into laminar-specific neural activity and functional connectivity. It can also help mitigate motion-related artefacts, as the acquisition of a single line is less susceptible to motion-induced blurring compared to full 3D volumes.

Line-scanning was introduced by Yu et al. in their pioneer study on rats, where they showed that the method allowed to perform high-resolution imaging of the hemodynamic response function across cortical layers<sup>51</sup>. These features enabled the authors to conclude that the onset of the hemodynamic response in the brain is not uniform across cortical layers, and the peak fMRI signal does not correspond to the onset time (Fig 2).

A more recent work by Raimondo et al. introduced a novel method for line-scanning fMRI at 7T to enhance spatial and temporal resolution.<sup>20</sup> They modified a pre-existing 2D GE-BOLD sequence by deactivating the phase-encoding gradients, causing the MR signal to collapse along the phase-encoding direction into a line profile (Fig 3A). As a result, each "phase-encoding step" in a traditional fMRI experiment now became a time point, converting the spatial information into a temporal function. To ensure high spatial specificity during line-scanning fMRI, the authors implemented outer volume suppression (OVS) using two saturation pulses (Fig 3A, 2D and 2E). These saturation slabs were placed strategically to suppress any undesired signal from outside the region of interest, particularly in the visual cortex. By applying the line-scanning method during a visual stimulation task, they measured the blood oxygen level-dependent (BOLD) responses along cortical depth every 250 mm with a 200 ms TR. The acquisition of k-space was performed using a line-scanning k-space sampling pattern (Fig B), acquiring the same frequency-encoding ( $k_{FE}$ ) line every TR. This approach demonstrated superior performance compared to the standard 2D GE-EPI method, offering reliable BOLD responses at sub-

millimetre and sub-second resolution. The study further examined the BOLD percentage signal change (PSC) across cortical depth and time within ROI (Fig 3G). The plot revealed varying magnitudes of neural response over both cortical depth and time, indicating distinct neural processes within different layers of the cortex. Additionally, the t-stats values (Fig 3H) showed the statistical significance of BOLD responses across cortical depth, with higher values observed in voxels containing grey matter, suggesting robust neural activity in this region. The line-scanning technique proved to be feasible in human subjects and holds promising applications in cognitive and clinical neuroscience (Fig 3I).

The same group made significant advancements in human line-scanning fMRI by introducing several improvements to the existing technique<sup>21</sup>. These enhancements included multi-echo readout, NORDIC denoising to reduce thermal noise levels, and prospective motion correction (Fig. 4A). By combining these methods, they achieved a substantial enhancement in data quality, evident in improved temporal signal-to-noise ratio (tSNR) and more robust t-statistical values. In particular, the researchers employed a 5-echo multi-echo acquisition method, which outperformed the previous single-echo line-scanning approach in terms of tSNR and t-statistical values. The application of NORDIC denoising effectively removed noise artefacts from the data, resulting in higher quality and more reliable measurements. The denoising process substantially improved the tSNR (Fig. 4D, 4E). NORDIC denoising not only improved t-stats but also preserved the BOLD response characteristics, enabling better detection of the BOLD response to the visual task (Fig. 4D, 4E).

Finally, the group explored the potential of a spin-echo line-scanning (SELINe) sequence (Fig. 5A)<sup>52</sup>. This novel sequence offered the promise of both high spatial and temporal resolution (250  $\mu$ m, 500 ms) and the advantage of microvascular specificity in functional responses. This specificity was crucial as the corresponding gradient-echo version (GELINe) often suffered from compromised sensitivity to changes in the local T2\* relaxation time. The authors found that SELINe displayed significantly improved line selection, evident from a sharper line profile compared to GELINe. However, this improvement came at the cost of a substantial drop in functional sensitivity. Precisely, the SELINe sequence employed two different orientations of 90° and 180° gradients for the excitation and refocusing of perpendicular planes (Fig. 4A). This selective excitation and refocusing of longitudinal modes allowed image-specific planes while minimizing unwanted signals from other planes (Fig. 5B). Overall, the SELINe sequence exhibited promising characteristics for high spatial and temporal resolution fMRI with microvascular specificity (Fig. 5). However, the challenge of low functional sensitivity needs to be addressed before fully harnessing its potential for neuroscientific applications.

However, line scanning poses several challenges. The reduced field of view limits the coverage of the brain, potentially missing important activations outside the scanned line<sup>20,21,52</sup>. Furthermore, careful consideration is needed when interpreting line-scanning results, as the

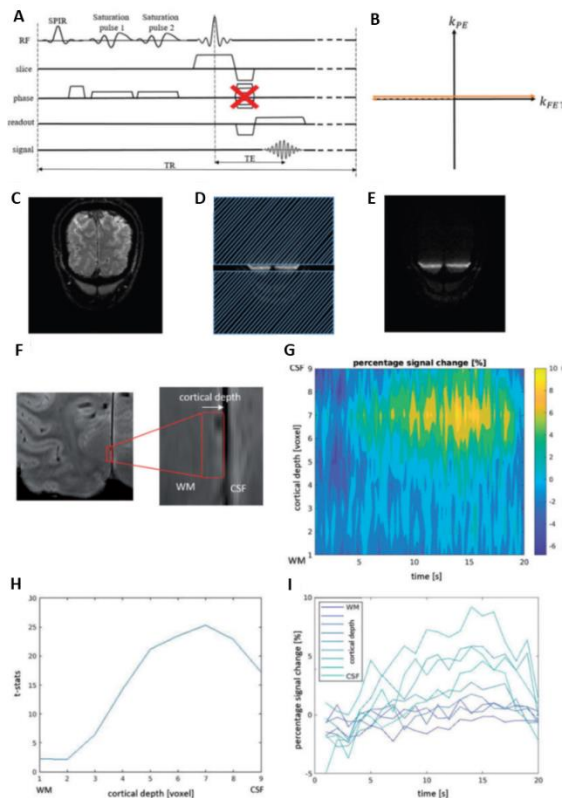


**Fig 3.** (A) Gradient echo line-scanning sequence with removed phase-encoding gradients and outer volume suppression slabs. (B) Line-scanning k-space sampling pattern, acquiring the same  $k_{FE}$  line every TR. (C) Slice obtained from the line-scanning sequence. (D) Outer volume suppression (OVS) using saturation slabs to minimize undesired signals outside the region of interest. (E) Effect of OVS on the phase-encoded slice, resulting in a cleaner and more focused image. (F) ROI indicated by a red box on the anatomical image, highlighting the specific cortical area under investigation. (G) BOLD percentage signal change (PSC) across cortical depth and time within the ROI, showing varying neural responses. (H) t-stats values indicating statistical significance of BOLD responses across cortical depth, with higher t-stats in gray matter voxels. (I) Mean PSC plotted against time, revealing distinct neural processes in different layers of the cortex<sup>20</sup>.

sampled line may not fully capture the complexity and spatial extent of functional activations<sup>49,50</sup>. Therefore, line scanning is often used in conjunction with other imaging techniques to provide complementary information about local cortical dynamics and connectivity. Overall, line-scanning offers a valuable approach for high-temporal-resolution investigations of specific cortical regions or layers, with advantages in motion mitigation and reduced physiological noise, while requiring careful interpretation and consideration of its limitations in coverage and spatial extent.

Despite its extensive sensitivity to changes in deoxyhemoglobin and wide accessibility, BOLD fMRI has several limitations. Spatial specificity is constrained due to the predominant influence of large draining vessels on the BOLD signal<sup>10,26</sup>. Images are subject to geometric distortions stemming from the lengthy EPI readout, and signal dropout can occur in regions near air cavities.

Finally, the BOLD signal does not directly or quantitatively measure brain function<sup>9,20,27,52</sup>.

#### 4. VASO-CBV

CBV signal is an alternative imaging contrast that offers a more comprehensive understanding of the neurovascular dynamics during task-based experiments<sup>9</sup>. Unlike traditional BOLD fMRI, which relies on changes in blood oxygenation, CBV fMRI focuses on variations in cerebral blood volume as an indicator of neural activity. By directly probing vascular responses associated with brain activation, CBV fMRI provides valuable insights into the interplay between neural and hemodynamic processes. CBF using VASO utilizes magnetization inversion to selectively null the signal from venous blood while preserving the signal from tissue and arterial blood<sup>26,53</sup>. This selective nulling allows VASO to measure tissue-based responses, making it particularly adept at studying small vascular structures and layer-dependent activity within the cortex. By enhancing the specificity of fMRI signals to tissue changes and minimizing the influence of large draining veins, VASO provides improved sensitivity to subtle neural activity variations.

Huber et al. conducted a study on optimal acceleration and reconstruction strategies for layer-dependent VASO fMRI<sup>53</sup>. They suggest that for ultra-high resolutions, alternative contrast mechanisms (e.g., CBV) and readout strategies (e.g., 3D-segmented-EPI) may be more advantageous than conventional functional contrast (GE-BOLD) and readout strategies (2D-EPI). Specifically, CBV with 3D-segmented EPI demonstrated superior signal stability and local specificity to cortical layers, making it a more suitable choice for neuroscientific layer-dependent applications compared to classical GE BOLD EPI.

In a more recent study, Huber et al. delved into the potential of layer-specific vascular-space-occupancy (VASO) fMRI to distinguish activation related to cortical input and output in the primary motor cortex (Fig. 6)<sup>54</sup>. They employed a 3D-VASO sequence based on a 3D-EPI implementation and parameters from a previous study, allowing them to measure input and output activity separately. The findings revealed that the non-invasive, CBV-weighted fMRI data accurately reflected neural activity in the cortical layers and showcased directional functional connectivity. This innovative technique provided an additional level of detail to conventional fMRI, enabling *in vivo* investigations of cortical micro-circuitry in both healthy individuals and those with neurological disorders. Moreover, it acted as a bridge between macroscopic (conventional fMRI) and microscopic (extracellular recordings) assessments of brain function. The motor cortex was the focal point of the study, and participants performed four different sensorimotor tasks. The averaged layer-dependent fMRI responses in all participants showed fMRI signals with variations according to cortical depth within the thumb-index finger pinch motor area (Fig. 6A). Furthermore, across all participants, the average cortical profiles displayed distinct laminar patterns in superficial and deep cortical laminae for each task (Fig. 6B). To ensure



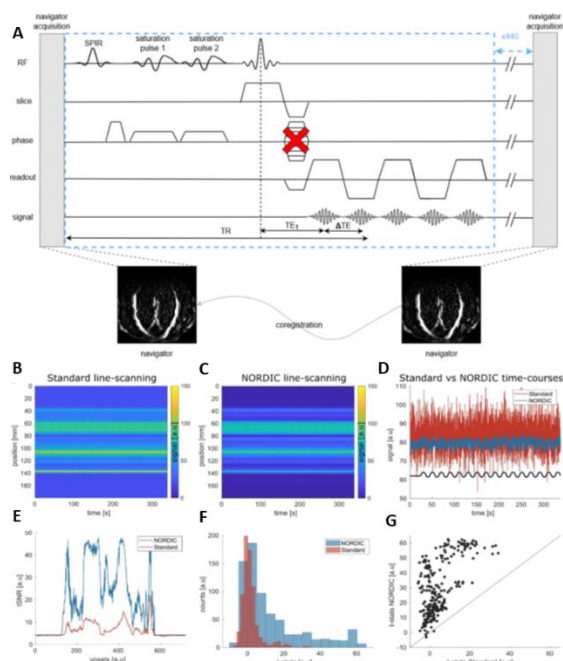


**Fig 4.** (A) Sequence diagram for prospective motion correction. (B) Standard line-scanning fMRI data. (C) The same data after undergoing NORDIC denoising, removing noise artifacts. (D) Single voxel timecourse for standard line-scanning data (red line) and NORDIC-denoised data (blue line) alongside the GLM model following the visual task. (E) Comparison of tSNR (temporal signal-to-noise ratio) between standard line-scanning data (red line) and NORDIC-denoised data (blue line), showing improved tSNR and higher data quality. (F) Distributions of t-stats for standard data (red) and NORDIC-denoised data (blue), highlighting enhanced t-stats distribution and more robust statistical results. (G) Scatter plot representing t-stats values for one participant, comparing standard and NORDIC-denoised t-stats. NORDIC denoising improves t-stats, leading to better detection of the BOLD response to the visual task while preserving BOLD response

accuracy, the shaded areas represented the standard error of the mean (SEM) across participants. Although the layer-specific VASO fMRI technique demonstrated promising results, the authors acknowledged that its universal applicability to all brain regions or tasks might be limited. Nonetheless, this research contributes valuable insights into understanding cortical processing and connectivity in the human brain.

Lately, Oliveira et al. conducted a study to explore the potential advantages of VASO-CBV imaging over BOLD imaging in terms of spatial specificity<sup>24</sup>. They utilized sub-millimetre resolution VASO fMRI at 7 T to simultaneously map VASO-CBV and BOLD responses in the motor and somatosensory cortices during individual finger movement tasks (Fig 7). The researchers evaluated the cortical overlap in two ways: first, by calculating similarity coefficient metrics (Dice and Jaccard), and second, by computing selectivity measures. The paper's results demonstrated that VASO-CBV responses exhibited less overlap between the digit clusters compared to BOLD, with higher selectivity measures for VASO-CBV. Additionally, the authors observed a consistent

topographical organization of the targeted digit representations (thumb-index-little finger) in the motor areas. These findings remained consistent across metrics and participants, confirming that VASO-CBV provided higher spatial specificity than BOLD. In their imaging protocol, a carefully positioned slab was used to encompass the left primary sensorimotor area (Fig. 7A). The participants engaged in a block-designed individual finger movement task (Fig. 7B). The digit representations were found to be organized in an orderly manner along the central sulcus, primarily within the S1 area, following the arrangement of fingers - thumb, index, and little finger (Fig. 7C). This precise mapping method allowed researchers to study the neural representations of the fingers in the primary sensorimotor area, leading to valuable insights into the topographic organization of digit representations in the brain.

In summary, CBV fMRI provides valuable insights into the interplay between neural and hemodynamic processes during task-based experiments. This integration enhances the specificity of fMRI signals, making it well-suited for studying small vascular structures and cortical layer-dependent activity, ultimately improving spatial specificity and advancing our comprehension of brain function and cognitive processes. Nevertheless, CBV techniques in fMRI come with certain limitations, such as lower signal-to-noise ratios, longer acquisition times, limited spatial coverage, reduced temporal resolution and high sensitivity to magnetic field strength. Despite these challenges, the potential benefits of CBV and VASO integration in advancing brain mapping and cognitive neuroscience research make them a promising avenue for future investigations. Addressing these limitations and refining the methodologies will be crucial for maximizing their potential in functional brain imaging studies.

## 5. ASL-CBF

CBF fMRI using ASL is an innovative and non-invasive technique that directly measures CBF in the brain<sup>27,28</sup>. Unlike traditional BOLD fMRI, ASL utilizes magnetically labelled arterial blood water as an endogenous contrast agent, providing a quantitative and more direct measure of neural activity<sup>55</sup>. This approach enables investigations at the layer and column levels, offering opportunities to study fine-scale neural structures and functional organization with improved precision. Further, ASL's interrogation of CBF changes provides valuable insights into the neurovascular coupling mechanisms underlying cognitive processes and the dynamics of cortical microcircuits, advancing our understanding of brain function at different spatial scales<sup>56</sup>. Despite lower SNR and acquisition speed, ASL's quantitative nature and temporal stability make it suitable for longer experimental paradigms, such as pharmacological fMRI and studying conditions like sleep deprivation. Moreover, ASL's specificity to CBF and CBV changes within the neural parenchyma makes it attractive for layer-specific fMRI, surpassing BOLD imaging in differentiating activity between cortical layers<sup>10,55</sup>. Additionally, ASL's advantages extend to regions with susceptibility-induced static field inhomogeneities, where BOLD techniques may

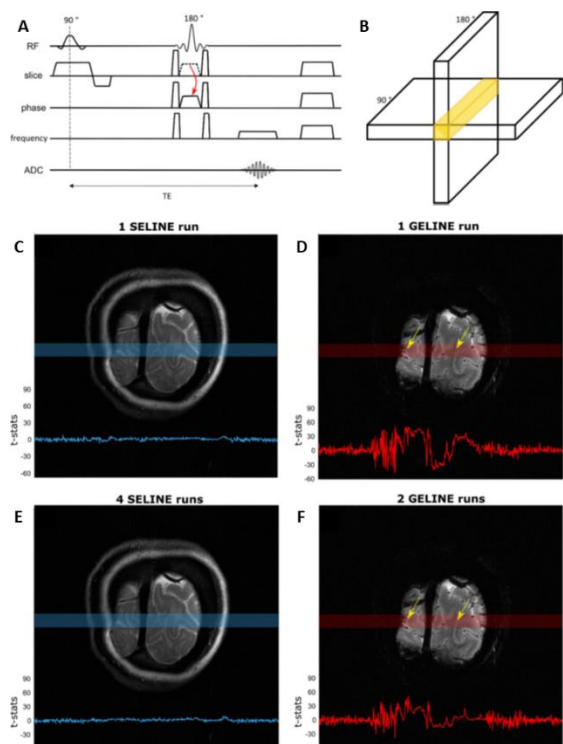


**Fig 5.** SELINE and GELINE sequence comparisons. (A) SELINE omits phase-encoding gradients, utilizing  $90^\circ$  and  $180^\circ$  gradients to excite and refocus perpendicular planes (red arrow). Crusher gradients prevent artifacts, while spoilers eliminate transverse magnetization. (B) Excitation and refocusing of two perpendicular planes (yellow beam), minimizing unwanted signals from other planes. (C) t-stats for 1 SELINE acquisition, (D) t-stats for 1 GELINE acquisition, showing statistical significance. (E) t-stats for 4 runs averaged SELINE acquisition, and (F) t-stats for 2 runs averaged GELINE acquisition, with t-stats overlaid on acquired slices. Light blue and red boxes show regions of line-scanning acquisitions for focused analysis in specific regions of interest<sup>52</sup>.

suffer from signal loss. ASL-based fMRI sequences, such as 3D stack of spirals and 3D-GRASE readouts, efficiently collect k-space data after a single labelling/control period, ensuring sufficient temporal resolution<sup>55</sup>.

At UHF, ASL benefits from increased intrinsic SNR and longer T1 relaxation times of blood, offering potential advantages in shorter scan times, higher spatial resolution, and improved sensitivity to low perfusion levels<sup>10,55</sup>. However, technical challenges have limited the widespread use of ASL at UHF, including increased  $B_0$  and  $B_1+$  inhomogeneity, higher power deposition, and increased  $T_2/T_2^*$  decay. Recent advances in optimized inversion pulses and SMS EPI have improved ASL labelling efficiency, brain coverage, and temporal resolution, making it promising for high spatial resolution functional imaging, such as laminar and columnar fMRI<sup>55</sup>. While pseudo continuous ASL (PCASL) offers potential solutions for whole-brain coverage, it remains sensitive to technical issues, necessitating further work to tackle these challenges<sup>56</sup>. Mitigating  $B_0$  inhomogeneity, compensating for reduced  $B_1+$  amplitude, and improving transmit efficiency are critical areas of investigation<sup>4,12</sup>. Overcoming these challenges could realize the full

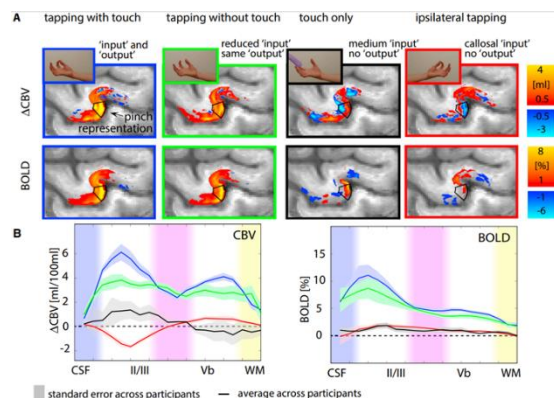


**Fig 6.** Layer-dependent fMRI responses in the motor cortex during four sensorimotor tasks. (A) Tasks in the thumb-index finger pinch motor area showed depth-related signal variations (black box). (B) Average cortical profiles across participants revealed distinct laminar patterns for each task. Shaded areas represent the standard error of the mean (SEM).

theoretical potential of ASL at UHF, enabling optimal labelling and background suppression and potentially utilizing full parallel transmission capabilities. UHF pulsed ASL (PASL) could be considered for very high spatial resolution needs, particularly for layer-specific functional imaging<sup>29,55,56</sup>. Moreover, in UHF task-based fMRI studies, common ASL settings involve the use of pseudo-continuous labelling schemes and 3D multi-slice acquisition techniques, providing robust and reliable CBF measurements and enhancing labelling efficiency and CBF sensitivity. Finally, the 3D multi-slice acquisition enables the simultaneous acquisition of multiple slices, improving temporal resolution and facilitating investigations of rapid neural dynamics with enhanced precision. By adopting these settings, UHF task-based ASL fMRI achieves enhanced spatial and temporal specificity, allowing for more precise examinations of brain function and cognitive processes.

## 6. Other Strategies

In the following sections, we will discuss alternative approaches to high spatiotemporal resolution fMRI, combining or adapting the techniques previously described, which yielded highly encouraging results. As certain techniques like CBV and CBF-weighted fMRI may have limitations in spatial specificity, we will also explore other methods like spin-echo EPI (SE-EPI)<sup>57,58</sup>, which, despite potential noise concerns compared to ASL or VASO fMRI, offers higher spatial specificity. By examining these different approaches and their respective strengths and weaknesses, we aim to provide insights that will help researchers make informed decisions in selecting the most suitable technique for their specific research needs, striking a balance between spatial and temporal considerations.

As anticipated, while GE-EPI remains the dominant fMRI method at UHF, spin-echo EPI (SE-EPI) has gained attention due to its potential advantages in mitigating susceptibility artefacts and improving functional

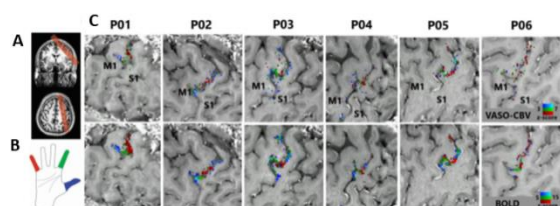


**Fig 7.** VASO-CBV and BOLD topographic digit mapping in six participants. (A) Imaging used a carefully positioned slab encompassing the left primary sensorimotor area. (B) Participants performed finger movement tasks, using their thumb (D1, blue), index finger (D2, green), and little finger (D5, red) in a block-designed manner. (C) Voxel data was assigned to specific digits using a winner-take-all algorithm, creating digit representation maps. Notably, representations followed an organized pattern along the central sulcus, predominantly within the S1 area, reflecting the finger arrangement - thumb, index, and little finger. This method precisely mapped neural representations of fingers in the primary sensorimotor area, providing valuable insights into the topographic organization of digit representations in the brain.

specificity<sup>57-59</sup>. SE-EPI incorporates a refocusing radio frequency (RF) pulse to create a SE, which reduces signal dropout caused by susceptibility effects. By acquiring both positive and negative contrast images, SE-EPI enables more accurate detection of the BOLD signal and differentiation between extravascular and intravascular contributions. Additionally, SE-EPI provides valuable insights into microvascular and macrovascular contributions to the BOLD signal, contributing to a better understanding of neurovascular coupling and addressing potential confounds associated with GE-EPI.

In early work by Yacoub et al., Hahn Spin Echo (HSE) BOLD functional MRI at 7 Tesla demonstrated reproducible mapping of ocular dominance columns (ODCs) in the human visual cortex with high accuracy and robustness<sup>60</sup>. This HSE BOLD methodology provided a more generalized approach for mapping cortical functional architecture compared to the conventional GE-BOLD signal, which sometimes struggled to uniformly resolve ODCs due to non-specific signals. By refocusing and suppressing BOLD effects caused by large vessels in the extravascular space, HSE BOLD signals mainly originated from the microvasculature, eliminating blood signals at high magnetic fields. This advancement holds promise for studying the functional architecture of human sensory cortices and specific cognitive processes. Despite the increased energy deposition in subjects, limiting volume coverage and temporal resolution, HSE BOLD remains a valuable tool for understanding cortical functional architecture and cognitive processes in the human brain.

In a recent study, Privolous et al. addressed the limited spatial specificity of BOLD fMRI caused by cortical depth-dependent venous bias, which hampers the exploration of cortical layers, columns, and signal directionality between brain regions<sup>61</sup>. To overcome this limitation, the researchers introduced a novel approach named Arterial Blood Contrast (ABC). This method selectively reduces venous and tissue signals using a pulsed saturation scheme, enhancing intracortical fMRI contrast based on CBV weighting (Fig. 8). The ABC

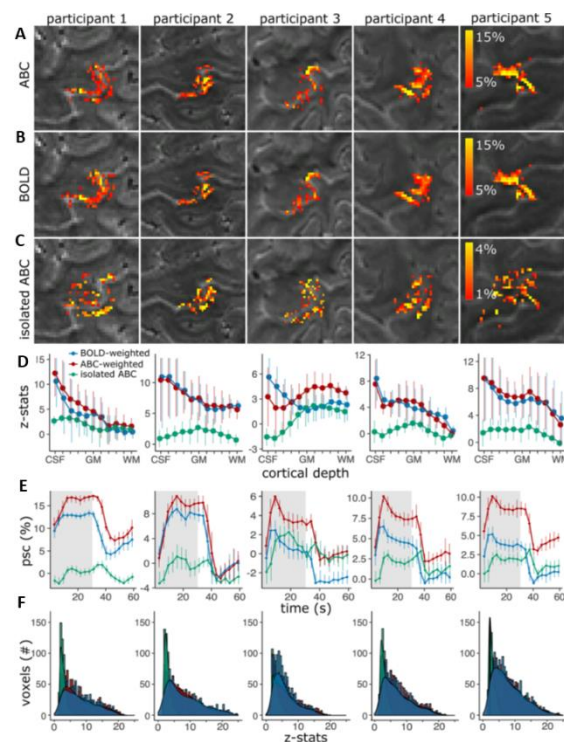


**Fig 8.** fMRI signal change analysis overview: (A) Unsmoothed fMRI signal change during right index hand flexing for participants, masked for M1 and S1. (B) BOLD fMRI signal change during the task, thresholded at 5% for significant responses. (C) Isolated-ABC signal change, thresholded at 1%. (D) Cortical depth analysis; isolated-ABC reduces pial-surface bias for accurate depth-dependent fMRI responses. (E) Mean timecourse of fMRI signal change in the region of interest. (F) z-stat distribution of significant voxels in M1 using different approaches: time-matched ABC (red), time-matched BOLD (blue), and isolated-ABC (green)<sup>61</sup>.

technique maintains high sensitivity and spatial resolution in humans while modulating the typical fMRI spatial specificity. To achieve a time-efficient ABC-weighted fMRI in the SAR-constrained 7 T environment, the authors combined a sparsely-repeated on-resonance magnetization transfer train with a centre-slice-out, submillimeter 3D-EPI, a technique that studies magnetization exchange between protons in free water and macromolecules in MRI. Additionally, they conducted an interleaved ABC and BOLD experiment to isolate the ABC component (Fig. 8C, 8D). Integrating ABC with the existing BOLD contrast effectively modulated intracortical contrast, while isolating the ABC component demonstrated a response free of pial-surface bias. The findings indicate the potential of ABC to enhance fMRI spatial specificity, opening up valuable applications in in-vivo neuroscience. Notably, a comparison with a recently introduced saturation-based arterial CBV-weighted method revealed that the ABC method displayed increased sensitivity to the more spatially-specific arterial and capillary CBV changes. These advancements represent a significant step towards advancing fMRI techniques and understanding brain function with greater precision.

To conclude, back in 2002, Silva et al. introduced an alternative method to increase temporal resolution in BOLD fMRI to the milliseconds scale<sup>62</sup>. They swapped



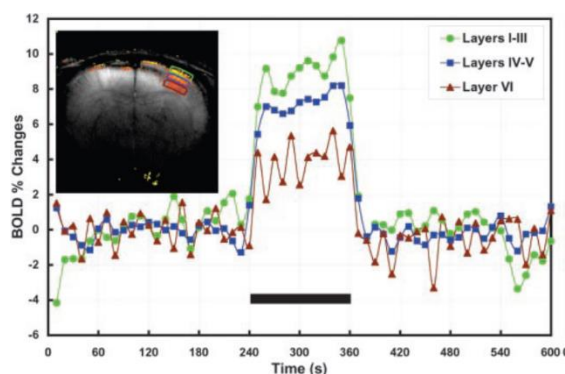


**Fig 9.** Laminar heterogeneity of BOLD signal changes with 10-second temporal resolution. Three BOLD time courses are shown for equal-sized ROIs representing different cortical layers: green (layers I–III), blue (layers IV–V), and brown (layer VI). The visual representation reveals diverse BOLD signal fluctuations across cortical layers during the stimulation period (black bar)<sup>62</sup>.

the order of the phase-encoding and repetition loop, acquiring one single k-space line for every time frame before incrementing the phase-encoding gradient to the next line (Fig 9). This approach reduced the TR down to 40 ms per frame, enabling the reliable detection of the onset time of BOLD signals. The study found that BOLD signal changes have distinct amplitude and temporal characteristics, varying spatially across cortical layers. The earliest onset time was found to correspond anatomically to layer IV, while superficial and deeper layers started significantly later. The research revealed considerable heterogeneity in the BOLD signal changes across the laminar organization of the brain, emphasizing the need to consider partial volume effects in oxygen consumption measurements. High temporal resolution fMRI may be more susceptible to noise and artefacts, potentially affecting measurement accuracy and increasing the risk of motion artefacts. However, the authors minimized the effects of physiological noise on the BOLD signal using a gated activation paradigm. They reported consistent results across different rats and cortical layers, indicating that the high temporal resolution was sufficient for their purposes. Fig. 9 shows the laminar heterogeneity of BOLD signal changes with a temporal resolution of 10 seconds per point. The BOLD time courses are displayed for three regions of interest (ROIs) based on the anatomical description of rat cortical layers. The top ROI encompasses pixels from layers I–III, the middle ROI comprises pixels from layers IV–V, and the bottom ROI includes pixels from layers VI. This visualization illustrates the diverse BOLD signal fluctuations across different cortical layers during the specified stimulation period.

DIANA (Direct Imaging of Neuronal Activity) is perhaps the latest and most exciting application of such a kind of sequence<sup>63</sup>. According to the authors, the method increases the temporal resolution up to the precision of neuronal activity in milliseconds while retaining the high spatial resolution of MRI by combining the line-scanning method previously discussed with the fast fMRI method explained above. Precisely, similarly to Silva and colleagues, the authors modified the 2D-GE sequence by

exchanging the phase-encoding and repetition loop to reach 5 ms resolution per frame by acquiring single k-space lines per stimulation period (Fig. 10). Further, they acquired data from a single 1-mm coronal brain slice (line) to obtain high spatial resolution. According to the study, this 2D fast line-scan method enabled direct imaging of neuronal activity with high temporal and spatial resolution. The results indicate the feasibility of DIANA through in vivo mouse brain imaging at 9.4 teslas during electrical whisker-pad stimulation. In vivo, spike recording and optogenetics confirmed the high correlation of the observed MRI signal with neuronal activity. Hence, the authors concluded that this convergence of high temporal and spatial resolution realized through DIANA could help elucidate the causal relationship between temporal and spatial dynamics of neural networks and their functions.

The authors found that the underlying mechanism of the DIANA response involves a strong T2 dependence, most likely resulting from changes in membrane potential leading to cell swelling and alterations in the hydration water of the plasma membrane. Additionally, the DIANA method ensures effective BOLD signal suppression with its extremely short TE, as the BOLD signal is typically optimal when  $TE \sim T2^*$ . These features suggest that the DIANA method may detect subtle magnetization changes on the neural surface during an action potential, providing direct access to highly-specific inter-neural communication. However, several limitations undermine DIANA. For instance, the DIANA sequence requires a high magnetic field strength (9.4T), which may limit its widespread use in clinical settings. Furthermore, the 2D Fast Line-Scan assumes consistent event-related responses across all trials without trial-by-trial variability, potentially introducing bias in the results with even small variations in neural spikes, given the method's high specificity. Lastly, although the study was conducted on mice, it remains unclear whether the same results can be obtained in humans, who exhibit more complex feedforward and feedback responses.

Finally, a recent study reported that the initial attempt to observe neuronal activation in humans using DIANA did not yield clear signals<sup>64</sup>. Although signals were detected that resembled possible functional activity when using small manually drawn ROI, increasing the stimulus duration did not lead to corroborating signal changes. Moreover, these signals disappeared when averaged over larger functionally or anatomically derived ROI. Further analysis of the data highlighted DIANA's sensitivity to inflow effects and subject motion. The paper concludes that the translation of DIANA from animals to humans appears to be non-trivial, and care should be taken not to mistake spurious signals for neuronal activity. The authors suggest that continued effort translating DIANA from mice to humans may well be worth it, considering the potential payoff. To aid in this endeavour, parallel studies focused on DIANA's biophysical underpinning and ability to detect excitatory and inhibitory signals in controlled settings will likely be of great value.

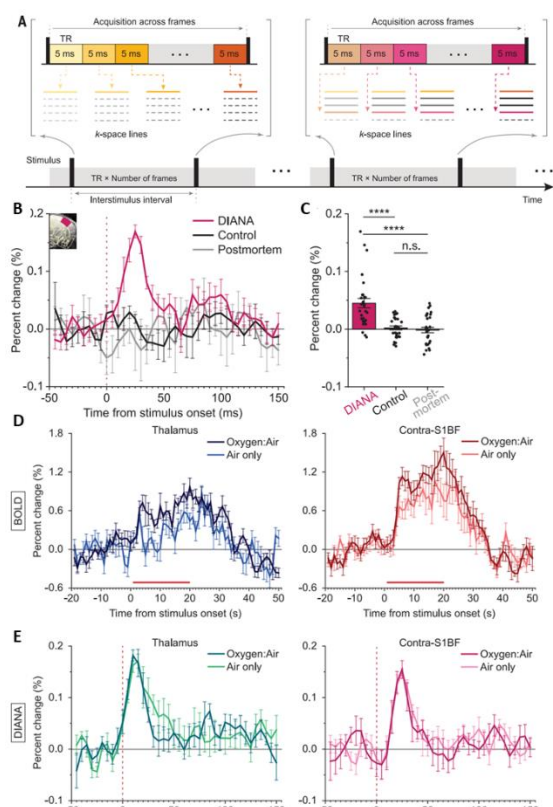


**Fig 10.** (A) 2D fast line-scan DIANA acquisition scheme for real-time visualization of neural activity. (B) Percent changes in DIANA signals reflecting neuronal responses to specific stimuli. (C) Mean signal changes during post-stimulation with electrical whisker-pad stimulation (magenta) and without stimulation (black). Also, postmortem condition shown in gray. (D) Percent signal changes of BOLD responses from thalamus (left) and contralateral S1BF (right) under two conditions. Red bar indicates electrical stimulation period. (E) Similar analysis using DIANA with data from six mice ( $n = 6$  mice). Vertical dashed lines indicate stimulation onset time for BOLD responses in thalamus and contralateral S1BF<sup>63</sup>.

## CONCLUSION

Task-based fMRI at UHF has revolutionized our understanding of the human brain, offering unprecedented precision in studying brain activity during specific cognitive tasks. Recent advancements in novel UHF fMRI techniques have significantly expanded our ability to explore neural responses and their relationship to cognitive processes, particularly in the realm of sub-millimetre fMRI, focusing on layer-dependent and column-dependent studies. By addressing the limitations of traditional BOLD fMRI methods, researchers have ventured into alternative contrast mechanisms, such as CBV imaging using VASO contrast and direct CBF measurements using ASL, providing promising avenues to study specific cortical layers and columns, revealing fine-scale neural structures and functional organization. Moreover, improvements in spatial resolution, like line-scanning fMRI, and enhanced temporal resolution through SMS acquisition have enabled more precise investigations of sub-millimetre structures and rapid neural dynamics.

These advancements not only offer valuable insights into the neural mechanisms underlying cognitive processes but also open the possibility for reliable mesoscopic resolution and sub-second temporal resolution in future fMRI studies. As the field of task-based UHF fMRI continues to evolve, the integration of these cutting-edge techniques with advancements in imaging hardware (e.g. surface coils and stronger static magnetic fields) and post-processing techniques (e.g. effective denoising) promises to unlock even more detailed and comprehensive understandings of brain function, opening new horizons for cognitive neuroscience research.

## ACKNOWLEDGEMENTS

I warmly thank Dr Wietske van der Zwaag for allowing me to conduct this assignment within her prestigious group in the Spinoza Centre for Neuroimaging under her precious and helpful supervision. Special thanks also to Dr Alex Bhogal for accepting to be the second reader and examiner of this not-so-exciting literature review in the middle of the summer.

## REFERENCES

- Heeger, D. J. & Ress, D. What does fMRI tell us about neuronal activity? *Nature Reviews Neuroscience* vol. 3 Preprint at <https://doi.org/10.1038/nrn730> (2002).
- Logothetis, N. K. What we can do and what we cannot do with fMRI. *Nature* vol. 453 Preprint at <https://doi.org/10.1038/nature06976> (2008).
- Sanjari Moghaddam, H. *et al.* A systematic review of resting-state and task-based fmri in juvenile myoclonic epilepsy. *Brain Imaging and Behavior* vol. 16 Preprint at <https://doi.org/10.1007/s11682-021-00595-5> (2022).
- Polimeni, J. R., Renvall, V., Zaretskaya, N. & Fischl, B. Analysis strategies for high-resolution UHF-fMRI data. *Neuroimage* **168**, (2018).
- Weldon, K. B. & Olman, C. A. Forging a path to mesoscopic imaging success with ultra-high field functional magnetic resonance imaging: Strategies for UHF fMRI. *Philosophical Transactions of the Royal Society B: Biological Sciences* vol. 376 Preprint at <https://doi.org/10.1098/rstb.2020.0040> (2021).
- Huettel, S. A. Event-related fMRI in cognition. *NeuroImage* vol. 62 Preprint at <https://doi.org/10.1016/j.neuroimage.2011.08.113> (2012).
- Yang, J., Gohel, S. & Vachha, B. Current methods and new directions in resting state fMRI. *Clinical Imaging* vol. 65 Preprint at <https://doi.org/10.1016/j.clinimag.2020.04.004> (2020).
- Moeller, S. *et al.* Multiband multislice GE-EPI at 7 tesla, with 16-fold acceleration using partial parallel imaging with application to high spatial and temporal whole-brain FMRI. *Magn Reson Med* **63**, (2010).
- Huber, L., Uludağ, K. & Möller, H. E. Non-BOLD contrast for laminar fMRI in humans: CBF, CBV, and CMRO2. *NeuroImage* vol. 197 Preprint at <https://doi.org/10.1016/j.neuroimage.2017.07.041> (2019).
- Borogovac, A. & Asllani, I. Arterial spin labeling (ASL) fMRI: Advantages, theoretical constraints and experimental challenges in neurosciences. *International Journal of Biomedical Imaging* vol. 2012 Preprint at <https://doi.org/10.1155/2012/818456> (2012).

11. Dumoulin, S. O., Fracasso, A., van der Zwaag, W., Siero, J. C. W. & Petridou, N. Ultra-high field MRI: Advancing systems neuroscience towards mesoscopic human brain function. *Neuroimage* **168**, (2018).
12. van der Zwaag, W., Schäfer, A., Marques, J. P., Turner, R. & Trampel, R. Recent applications of UHF-MRI in the study of human brain function and structure: a review. *NMR in Biomedicine* vol. 29 Preprint at <https://doi.org/10.1002/nbm.3275> (2016).
13. Logothetis, N. K. & Pfeuffer, J. On the nature of the BOLD fMRI contrast mechanism. in *Magnetic Resonance Imaging* vol. 22 (2004).
14. Laumann, T. O. *et al.* On the Stability of BOLD fMRI Correlations. *Cerebral Cortex* **27**, (2017).
15. Niranjana, A., Christie, I. N., Solomon, S. G., Wells, J. A. & Lythgoe, M. F. fMRI mapping of the visual system in the mouse brain with interleaved snapshot GE-EPI. *Neuroimage* **139**, (2016).
16. Feinberg, D. A., Cvetesic, N. & Beckett, A. Pushing the limits of ultra-high resolution human brain imaging with SMS-EPI demonstrated for columnar level fMRI. *Neuroimage* **164**, (2018).
17. Risk, B. B., Kociuba, M. C. & Rowe, D. B. Impacts of simultaneous multislice acquisition on sensitivity and specificity in fMRI. *Neuroimage* **172**, (2018).
18. Chu, A. & Noll, D. C. Coil compression in simultaneous multislice functional MRI with concentric ring slice-GRAPPA and SENSE. *Magn Reson Med* **76**, (2016).
19. Chiew, M. & Miller, K. L. Improved statistical efficiency of simultaneous multi-slice fMRI by reconstruction with spatially adaptive temporal smoothing. *Neuroimage* **203**, (2019).
20. Raimondo, L. *et al.* A line through the brain: implementation of human line-scanning at 7T for ultra-high spatiotemporal resolution fMRI. *Journal of Cerebral Blood Flow and Metabolism* **41**, (2021).
21. Raimondo, L. *et al.* Robust high spatio-temporal line-scanning fMRI in humans at 7T using multi-echo readouts, denoising and prospective motion correction. *J Neurosci Methods* **384**, (2023).
22. Schnell, G., Duenow, U. & Seitz, H. Effect of laser pulse overlap and scanning line overlap on femtosecond laser-structured Ti6Al4V surfaces. *Materials* **13**, (2020).
23. Hoxworth, J. M. *et al.* Performance of standardized relative CBV for quantifying regional histologic tumor burden in recurrent high-grade glioma: Comparison against normalized relative CBV using image-localized stereotactic biopsies. *American Journal of Neuroradiology* **41**, (2020).
24. de Oliveira, Í. A. F., Siero, J. C. W., Dumoulin, S. O. & van der Zwaag, W. Improved Selectivity in 7 T Digit Mapping Using VASO-CBV. *Brain Topogr* **36**, (2023).
25. Oliveira, Í. A. F. *et al.* Comparing BOLD and VASO-CBV population receptive field estimates in human visual cortex. *Neuroimage* **248**, (2022).
26. Huber, L. (Renzo) *et al.* Validating layer-specific VASO across species. *Neuroimage* **237**, (2021).
27. Zhang, X. *et al.* Quantitative basal CBF and CBF fMRI of rhesus monkeys using three-coil continuous arterial spin labeling. *Neuroimage* **34**, (2007).
28. Wey, H. Y., Wang, D. J. & Duong, T. Q. Baseline CBF, and BOLD, CBF, and CMRO<sub>2</sub> fMRI of visual and vibrotactile stimulations in baboons. *Journal of Cerebral Blood Flow and Metabolism* **31**, (2011).
29. Zhu, S., Fang, Z., Hu, S., Wang, Z. & Rao, H. Resting State Brain Function Analysis Using Concurrent BOLD in ASL Perfusion fMRI. *PLoS One* **8**, (2013).
30. Halai, A. D., Welbourne, S. R., Embleton, K. & Parkes, L. M. A comparison of dual gradient-echo and spin-echo fMRI of the inferior temporal lobe. *Hum Brain Mapp* **35**, (2014).
31. Yablonskiy, D. A. & Sukstanskii, A. L. Effects of biological tissue structural anisotropy and anisotropy of magnetic susceptibility on the gradient echo MRI signal phase: theoretical background. *NMR in Biomedicine* vol. 30 Preprint at <https://doi.org/10.1002/nbm.3655> (2017).
32. Caballero-Gaudes, C. & Reynolds, R. C. Methods for cleaning the BOLD fMRI signal. *Neuroimage* **154**, (2017).
33. Pais-Roldán, P., Yun, S. D. & Shah, N. J. Pre-processing of Sub-millimeter GE-BOLD fMRI Data for Laminar Applications. *Frontiers in Neuroimaging* **1**, (2022).
34. Kashyap, S. *et al.* Resolving laminar activation in human V1 using ultra-high spatial resolution fMRI at 7T. *Sci Rep* **8**, (2018).
35. Poser, B. A. & Norris, D. G. Investigating the benefits of multi-echo EPI for fMRI at 7 T. *Neuroimage* **45**, (2009).
36. Bhavsar, S., Zvyagintsev, M. & Mathiak, K. BOLD sensitivity and SNR characteristics of parallel imaging-accelerated single-shot multi-echo EPI for fMRI. *Neuroimage* **84**, (2014).
37. Fernandez, B., Leuchs, L., Sämman, P. G., Czisch, M. & Spoormaker, V. I. Multi-echo EPI of human fear conditioning reveals improved BOLD detection in ventromedial prefrontal cortex. *Neuroimage* **156**, (2017).
38. Vannesjo, S. J., Clare, S., Kasper, L., Tracey, I. & Miller, K. L. A method for correcting breathing-induced field fluctuations in T2\*-weighted spinal cord imaging using a respiratory trace. *Magn Reson Med* **81**, (2019).
39. Chen, N. K. & Wyrwicz, A. M. Correction for EPI distortions using multi-echo gradient-echo imaging. *Magn Reson Med* **41**, (1999).
40. Kundu, P., Inati, S. J., Evans, J. W., Luh, W. M. & Bandettini, P. A. Differentiating BOLD and non-BOLD signals in fMRI time series using multi-echo EPI. *Neuroimage* **60**, (2012).
41. Zahneisen, B., Poser, B. A., Ernst, T. & Stenger, A. V. Simultaneous Multi-Slice fMRI using spiral trajectories. *Neuroimage* **92**, (2014).
42. Pruessmann, K. P., Weiger, M., Scheidegger, M. B. & Boesiger, P. SENSE: Sensitivity encoding for fast MRI. *Magn Reson Med* **42**, (1999).
43. Mintzopoulos, D. *et al.* fMRI Using GRAPPA EPI with High Spatial Resolution Improves BOLD Signal Detection at 3T. *The Open Magnetic Resonance Journal* **2**, (2009).
44. Blaimer, M. *et al.* 2D-GRAPPA-operator for faster 3D parallel MRI. *Magn Reson Med* **56**, (2006).
45. Le Ster, C. *et al.* Comparison of SMS-EPI and 3D-EPI at 7T in an fMRI localizer study with matched spatiotemporal resolution and homogenized excitation profiles. *PLoS One* **14**, (2019).
46. Norbeck, O. *et al.* Optimizing 3D EPI for rapid T1-weighted imaging. *Magn Reson Med* **84**, (2020).
47. Jorge, J., Figueiredo, P., van der Zwaag, W. & Marques, J. P. Signal fluctuations in fMRI data acquired with 2D-EPI and 3D-EPI at 7 Tesla. *Magn Reson Imaging* **31**, (2013).
48. Van Der Zwaag, W. *et al.* Temporal SNR characteristics in segmented 3D-EPI at 7T. *Magn Reson Med* **67**, (2012).
49. Choi, S. *et al.* Laminar-specific functional connectivity mapping with multi-slice line-scanning fMRI. *Cerebral Cortex* **32**, (2022).

50. Albers, F., Schmid, F., Wachsmuth, L. & Faber, C. Line scanning fMRI reveals earlier onset of optogenetically evoked BOLD response in rat somatosensory cortex as compared to sensory stimulation. *Neuroimage* **164**, (2018).
51. Yu, X., Qian, C., Chen, D. Y., Dodd, S. J. & Koretsky, A. P. Deciphering laminar-specific neural inputs with line-scanning fMRI. *Nat Methods* **11**, 55–58 (2014).
52. Raimondo, L. *et al.* Towards functional spin-echo BOLD line-scanning in humans at 7T. *Magnetic Resonance Materials in Physics, Biology and Medicine* **36**, (2023).
53. Huber, L. *et al.* *Techniques for blood volume fMRI with VASO: From low-resolution mapping towards sub-millimeter layer-dependent applications.*
54. Huber, L. *et al.* High-Resolution CBV-fMRI Allows Mapping of Laminar Activity and Connectivity of Cortical Input and Output in Human M1. *Neuron* **96**, (2017).
55. Hernandez-Garcia, L. *et al.* Recent Technical Developments in ASL: A Review of the State of the Art. *Magnetic Resonance in Medicine* vol. 88 Preprint at <https://doi.org/10.1002/mrm.29381> (2022).
56. Dolui, S. *et al.* Comparison of PASL, PCASL, and background-suppressed 3D PCASL in mild cognitive impairment. *Hum Brain Mapp* **38**, (2017).
57. De Martino, F. *et al.* Spin echo functional MRI in bilateral auditory cortices at 7T: An application of B1 shimming. *Neuroimage* **63**, (2012).
58. Kemper, V. G. *et al.* Sub-millimeter T2 weighted fMRI at 7 T: Comparison of 3D-GRASE and 2D SE-EPI. *Front Neurosci* **9**, (2015).
59. Wang, J. *et al.* Reduced susceptibility effects in perfusion fMRI with single-shot spin-echo EPI acquisitions at 1.5 Tesla. *Magn Reson Imaging* **22**, (2004).
60. Yacoub, E., Shmuel, A., Logothetis, N. & Ugurbil, K. Robust detection of ocular dominance columns in humans using Hahn Spin Echo BOLD functional MRI at 7 Tesla. *Neuroimage* **37**, (2007).
61. Priovoulos, N., de Oliveira, I. A. F., Poser, B. A., Norris, D. G. & van der Zwaag, W. Combining arterial blood contrast with BOLD increases fMRI intracortical contrast. *Hum Brain Mapp* **44**, (2023).
62. Silva, A. C. & Koretsky, A. P. Laminar specificity of functional MRI onset times during somatosensory stimulation in rat. *Proc Natl Acad Sci U S A* **99**, (2002).
63. Tan Toi, P. *et al.* *In vivo direct imaging of neuronal activity at high temporospatial resolution.* <https://www.science.org> (2022).
64. Hodono, S., Rideaux, R., van Kerkoerle, T. & Cloos, M. A. Initial experiences with Direct Imaging of Neuronal Activity (DIANA) in humans. (2023).